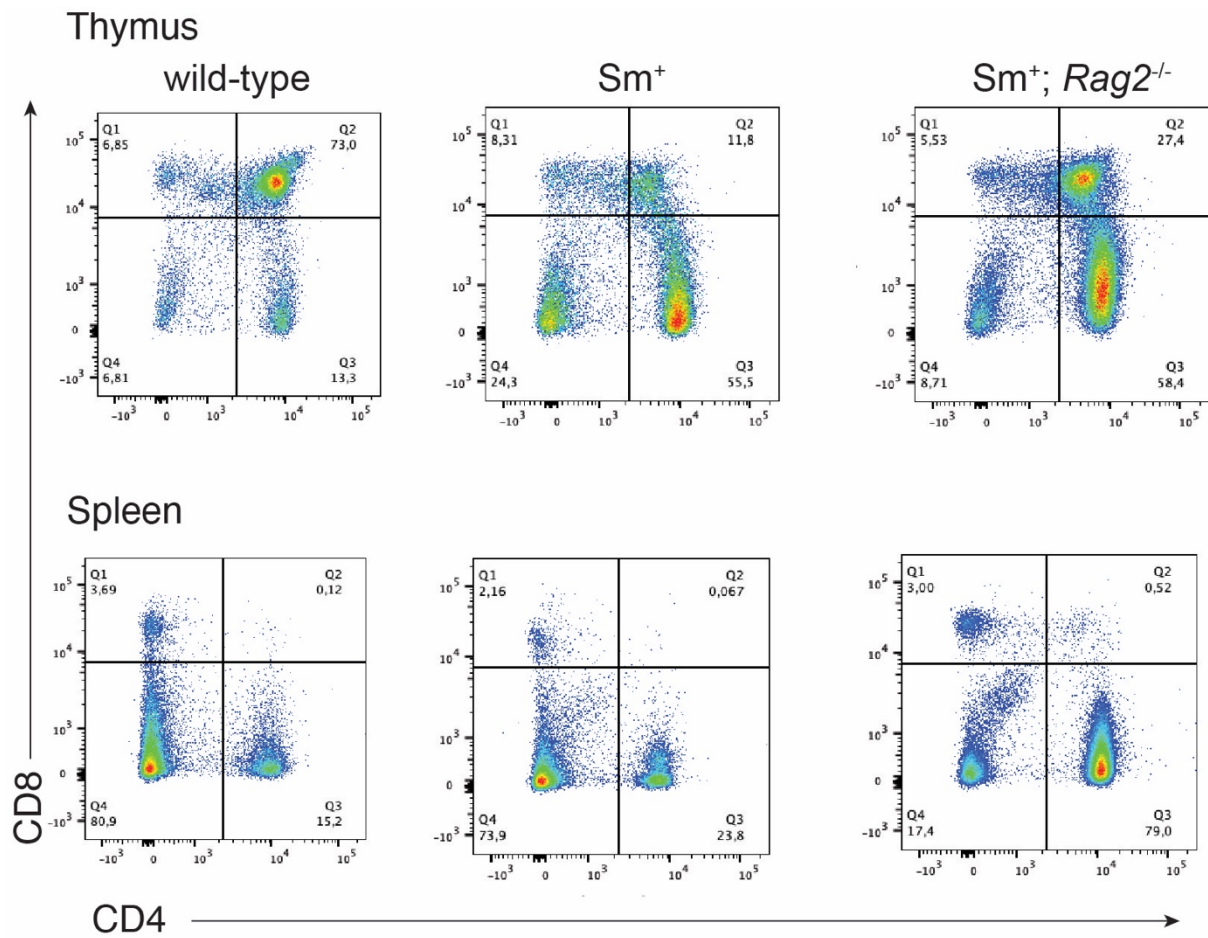


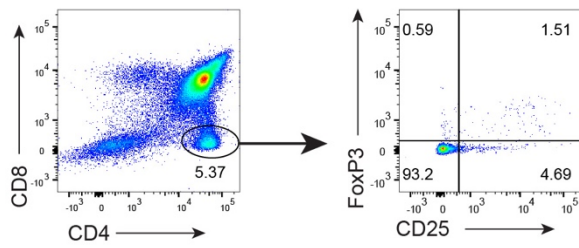
Supplementary Material
for
Probing TCR specificity using artificial in vivo diversification of CDR3 regions

Orlando B. Giorgetti, Annette Haas-Assenbaum and Thomas Boehm

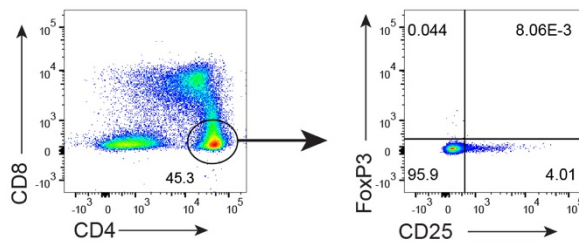


Supplementary Figure 1. Overall phenotype of Sm transgenic mice. Presence of CD4 single-positive and CD8 single-positive populations in non-transgenic wildtype, Sm transgenic, and Sm transgenic mice on the $Rag2$ -deficient background. Shown are representative profiles for thymocytes (top panels), and splenic lymphocytes (bottom panels).

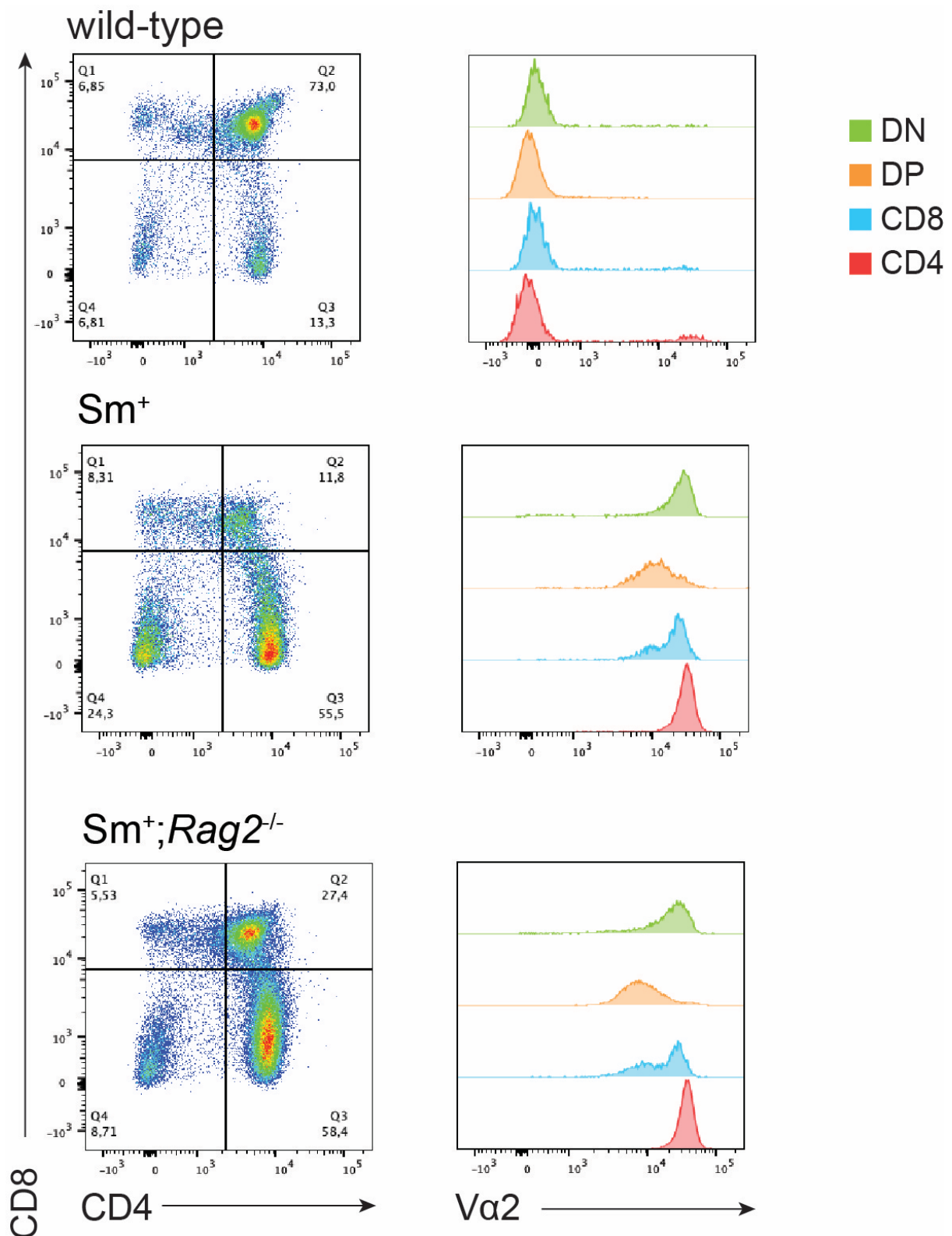
wild-type



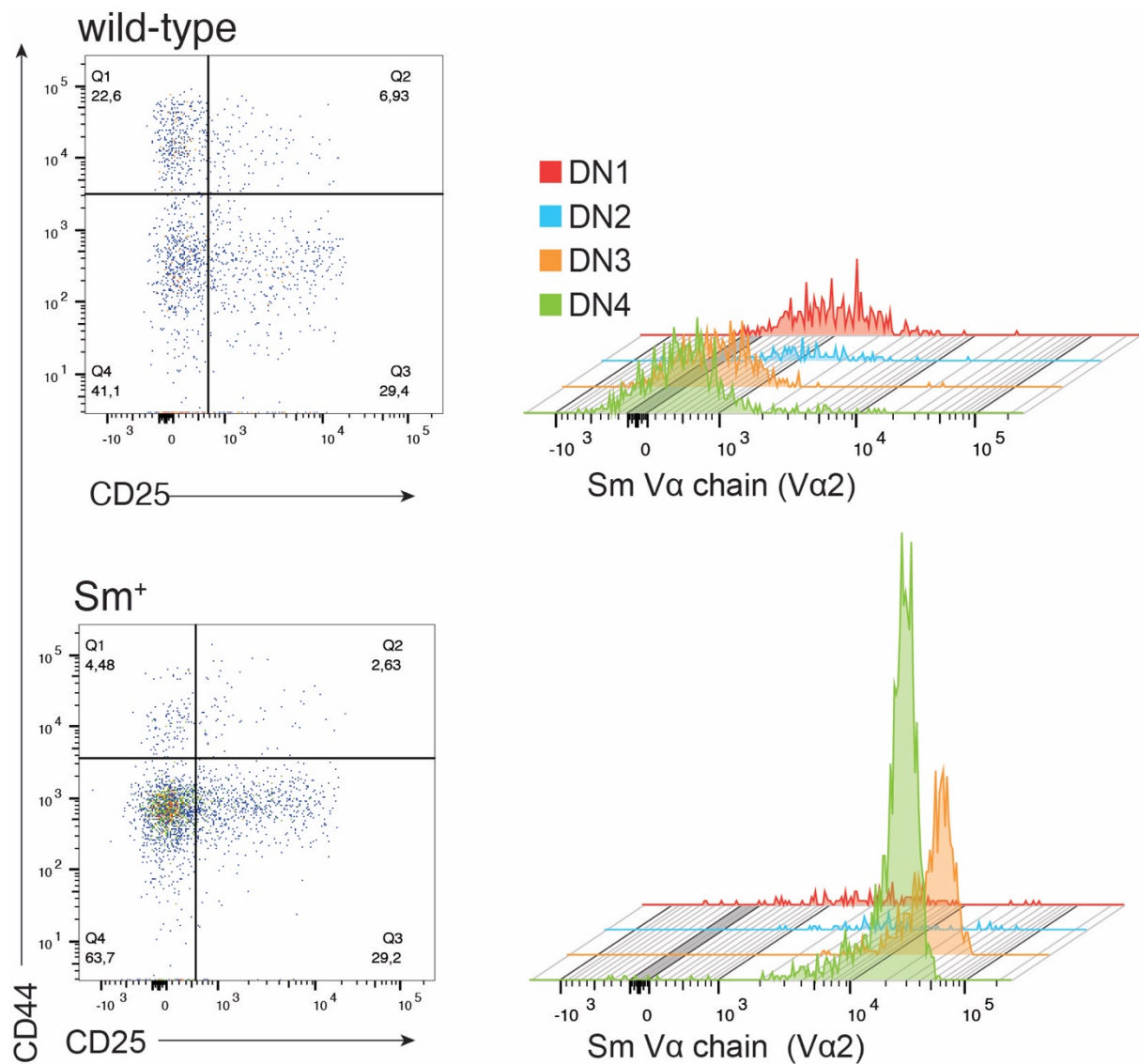
Sm⁺;Rag2^{-/-}



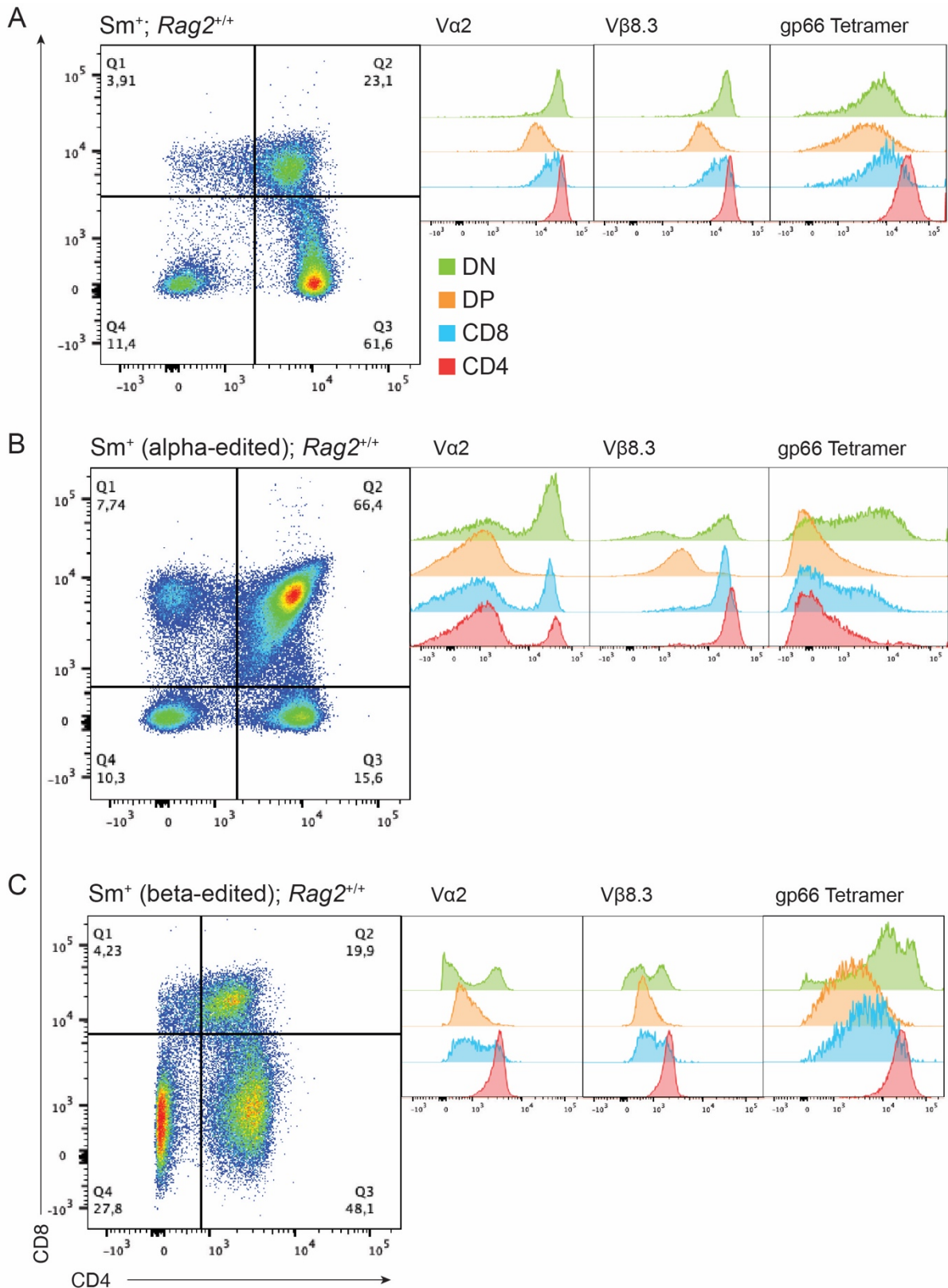
Supplementary Figure 2. Lack of Foxp3-positive cells in Sm transgenic mice. In CD4 single-positive thymocytes of wild-type mice, Foxp3-positive cells are readily detectable (upper panels), whereas no such cells are present in Sm transgenic mice on the *Rag2*-deficient background (bottom panels).



Supplementary Figure 3. Expression pattern of the transgenic V α 2 chain in the four major thymocyte populations. Thymocytes of mice with the indicated genotypes were separated according to CD4 and CD8 surface expression and analyzed for expression of the transgenic TCR V α 2 chain.



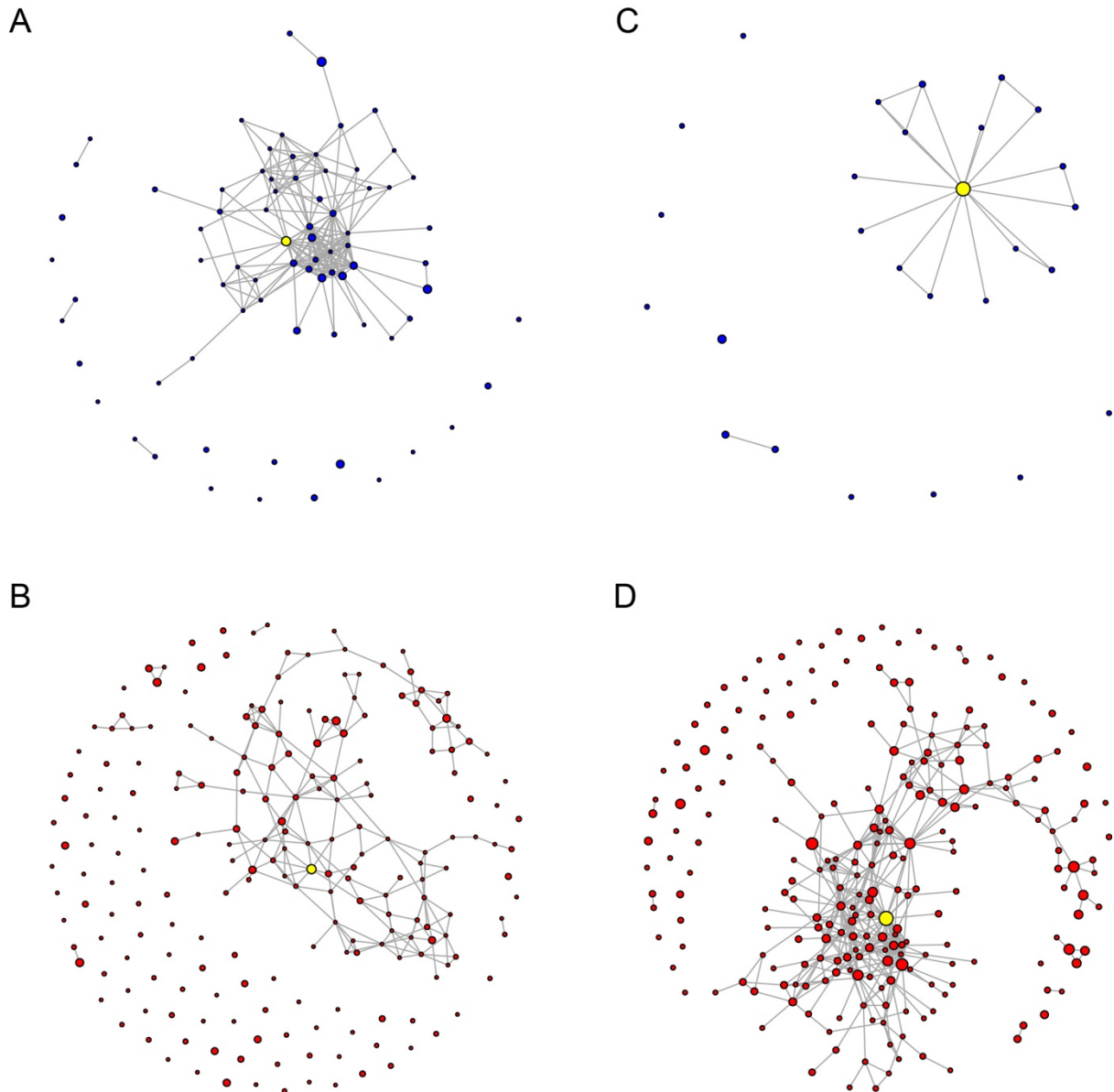
Supplementary Figure 4. Expression pattern of the transgenic Vα2 chain in the four DN thymocyte populations. Note that the transgenic TCR is first expressed at the DN3 stage, during which the *pLck:Cre* transgene is also active.



Supplementary Figure 5. Tetramer reactivity in the four major thymocyte populations.

(A) Detection of *Sm* TCR by antibodies directed against the cognate Va2 and Vβ8.3 regions, and a gp66-specific tetramer. (B) Detection of *Sm* TCR by antibodies directed against the cognate Va2 and Vβ8.3 regions, and a gp66-specific tetramer in *Tcrα*-edited mice in a *Rag2*-

sufficient background. Note the discrepancy between the V α /V β regions staining profiles and that of the tetramer; this outcome is to be expected if the editing of the *Tera* chain gene eliminates antigen reactivity, hence indicating efficient editing of the *Tera* CDR3 sequence. Efficient editing also leads to reversal of the distorted CD4/CD8 ratio. (C) Detection of Sm TCR by antibodies directed against the cognate V α 2 and V β 8.3 regions, and a gp66-specific tetramer in *Tcrb*-edited mice in a *Rag2*-sufficient background. Largely overlapping V α /V β and tetramer staining profiles suggest that, at the end of the selection process, most cells carry the unedited *Tcrb* sequence; this indicates that in order to survive positive selection in the thymus, only minor variations (if any) are tolerated in the *Tcrb* CDR3 region.



Supplementary Figure 6. Analysis of clonotypic networks in *TcrA*-edited and *TcrB*-edited peripheral CD4⁺ T cells. (A) Network depiction of amino acid CDR3 diversity of tetramer-positive cells in *TcrA*-edited mice. Sequences (nodes) that differ by a single amino acid from one another are connected by an edge. Node size is depicted on a logarithmic scale proportional to the UMI count. The original sequence is indicated as a yellow node. (B) Network depiction of amino acid CDR3 diversity of tetramer-negative cells in *TcrA*-edited mice. Conventions follow that for panel A. (C) Network depiction of amino acid CDR3 diversity of tetramer-positive cells in *TcrB*-edited mice. Conventions follow that for panel a. (D) Network depiction of amino acid CDR3 diversity of tetramer-negative cells in *TcrB*-edited mice. Conventions follow that for panel A.